Application of Mathematical Models to the Continuous Slab Casting Mold

B.G. Thomas
Department of Mechanical and Industrial Engineering
University of Illinois at Urbana-Champaign
Urbana, IL

This paper is reprinted from the 72nd Steelmaking Conference Proceedings April 2-5, 1989, Chicago, IL

ABSTRACT

Finite-element models have been developed to simulate fluid flow, heat transfer and stress generation in the mold region of a continuous steel slab casting machine. Using the separate models, it is now possible to calculate the turbulent fluid flow distribution and accompanying heat transfer resulting in the liquid steel delivered through a submerged, bifurcated nozzle; thermal distortion of the copper mold; and coupled heat flow, shrinkage and stress development in the solidifying steel shell. The model calculations have been compared with observations of physical water models and experimental measurements, and have successfully reproduced many known phenomena, in addition to making other new and interesting predictions. They are currently being applied to investigate problems such as narrow face shell erosion and slab surface depressions. Taken together, these models represent a powerful tool for gaining insight into the continuous casting process and the defects that can arise.

INTRODUCTION

Despite intensive study and several decades of commercial production, the continuous casting of steel is still plagued by many problems that are not fully understood. This is due, in part, to the complexity of the continuous casting process, which involves intimate interaction between such diverse phenomena as turbulent fluid flow, thermal convection, conduction, solidification, thermal contraction, phase transformations, plastic flow and creep, stress generation and microstructural changes including changing thermophysical and thermomechanical properties.

To assist in the understanding of this process, both physical and mathematical models have been developed and used extensively. However, the mathematical models that have been employed to date all have been limited by the need to make imperfect, simplifying assumptions. Even now, the computational complexity of the problem still prohibits the desirable, fully three-dimensional model that would couple together fluid flow, heat transfer and stress generation. Figure 1 draws attention to just some of the important aspects of this process that make it difficult to model:

(1) The four separate pieces of the mold that are clamped together and distort at elevated operating temperatures
(2) Turbulent fluid flow delivering heat to the growing shell
(3) Melting mold powder that mostly fills the interfacial gap, caused by
(4) Shrinkage of the shell away from the mold, especially near the corners
(5) Deformation of the weak shell under thermal and ferrostatic loading, both within the mold and between guide rolls after exiting

The recent increase in the power of modern computers is making it possible to extend the capabilities of mathematical models and to incorporate and investigate effects, such as those mentioned above, that were not possible previously. With a corresponding improvement in the control of the continuous casting process, the new insights gained through modeling could pay off in quality and productivity improvements. In addition, these models can readily be applied to the many novel casting processes that hold great promise for the future production of near net shapes.

This paper will summarize some recent work to develop advanced mathematical models of the continuous steel slab casting process, and apply them to gain insight into the complex phenomena that occur in the mold region and initiate surface defects. A brief discussion will be given of three separate models: turbulent fluid flow and heat transfer inside the continuous casting mold, thermal distortion of the mold itself and coupled heat transfer and stress generation in the solidifying shell.

MODEL OF FLUID FLOW AND HEAT FLOW WITHIN THE LIQUID POOL

The velocity distribution of the molten steel contained within the solidifying shell of a continuous casting

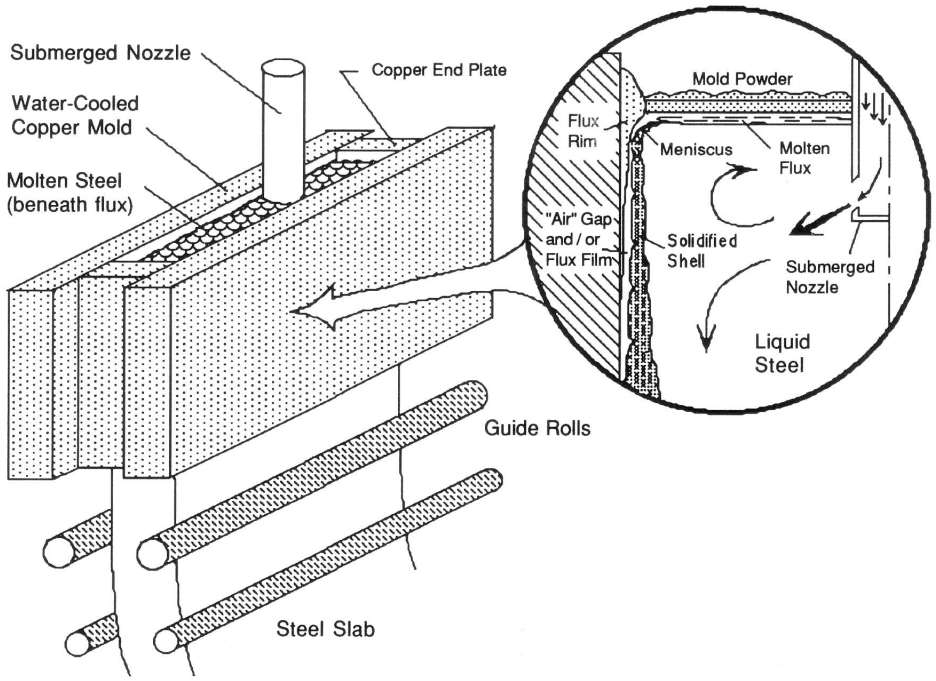

Fig. 1 — Schematic of continuous steel slab caster showing mold, fluid flow and shell growth.

machine is very influential on the distribution of inclusion particles, which is important to the internal cleanliness and quality of the steel. In addition, the flow pattern has a great influence on heat transfer to the shell during the critical initial stages of solidification. To further understand this behavior, a finite-element model has been developed to calculate both fluid flow and heat transfer of molten steel within the liquid pool inside the shell in the mold region of a continuous slab casting machine, fed by a bifurcated, submerged entry nozzle.

Model Formulation

Figure 2 illustrates the two-dimensional vertical section (parallel to the wide face through the center of the caster) and example mesh used by the model. This domain was chosen because the bifurcated nozzles used in slab casters combined with the high aspect ratio of the slab mold, produce flow patterns whose predominant characteristics are exhibited in these two dimensions. A fully three-dimensional model is currently under development, but requires more than an order of magnitude increase in computer time. Various slab caster lengths and widths have been simulated, exploiting symmetry about the center line of the caster, which is the left side of the model domain. The right side is the inside of the "narrow face" of the solidifying steel shell, which is adjacent to the mold at the top. Liquid steel enters the model domain through an inlet surface which represents a nozzle port. To determine the proper boundary conditions through this inlet surface from the nozzle port, a separate calculation is performed using a finite-element model of the nozzle itself.

This steady-state, turbulent fluid flow and heat transfer problem is described mathematically by the differential equations for continuity, momentum and energy conservation. In addition to solving these equations, the model also incorporates the popular two-equation "K-epsilon" turbulence model[1] to handle the fully turbulent, recirculating flow involved in this problem and wall equations to account for the laminar boundary layer. These equations have been used previously to simulate a variety of turbulent flows.[2-7] They handle the prohibitively small time and length scales of true turbulence by instead defining turbulence in terms of the averaged quantities of turbulent kinetic energy, K, and the turbulent dissipation, ε, which are then solved for as unknowns simultaneously with the velocity components. Since bouyancy effects due to the influence of temperature on the velocity fields are generally small, the energy equation can be uncoupled from the other equations. Temperatures are then calculated from the previous velocity solution. Only single-phase flow can currently be assumed, so effects such as those from argon gas bubble injection must await future model enhancements.

The present problem has been solved iteratively using the commercial code, FIDAP[8] with relaxed, successive substitution, and requires about 8 h of execution time on a Ridge 32S computer, or 7 CPU min on a Cray X/MP. This finite-element program is capable of simulating three-dimensional turbulent fluid flow coupled with heat transfer and has advantages over other finite-difference-based programs in handling arbitrary, complex geometries, such as found in the nozzle. Further details regarding the solution procedure can be found elsewhere.[8-10]

Physical modelers have long known that the nozzle delivering fluid to the domain of interest imparts important effects on the flow, so it must be modeled as well. Figure 3 shows how it is vital to include the nozzle in the mathematical simulation also. The four quite different flow patterns in this figure were all calculated assuming that the fluid entered the mold at an angle of 15 deg downward from horizontal at a casting speed of 1 m/min. The only difference between the simulations was the K and ε boundary

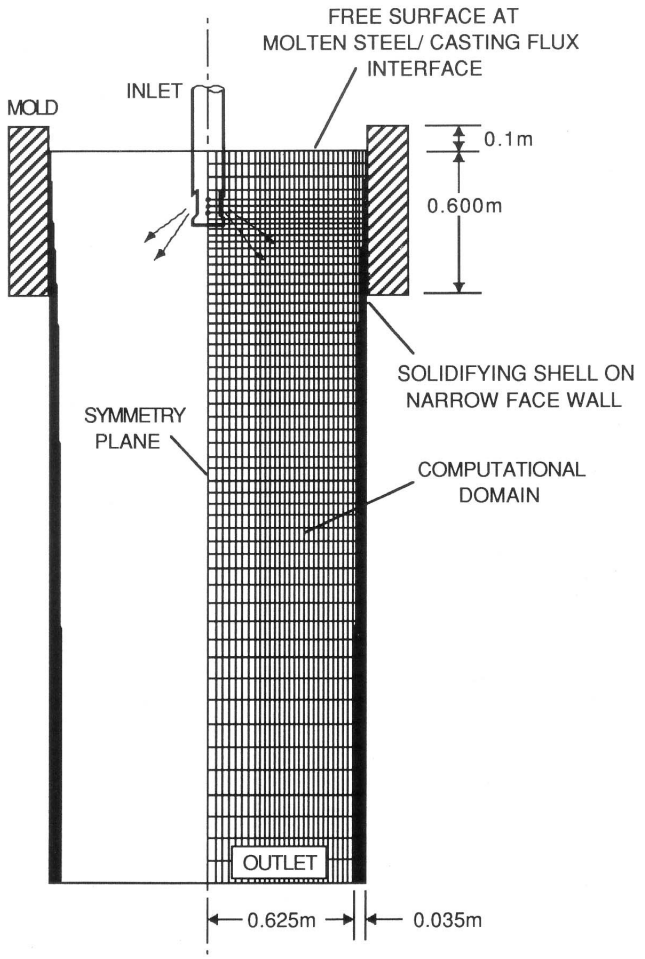

Fig. 2 — Simulation domain and mesh used in the fluid flow calculations.

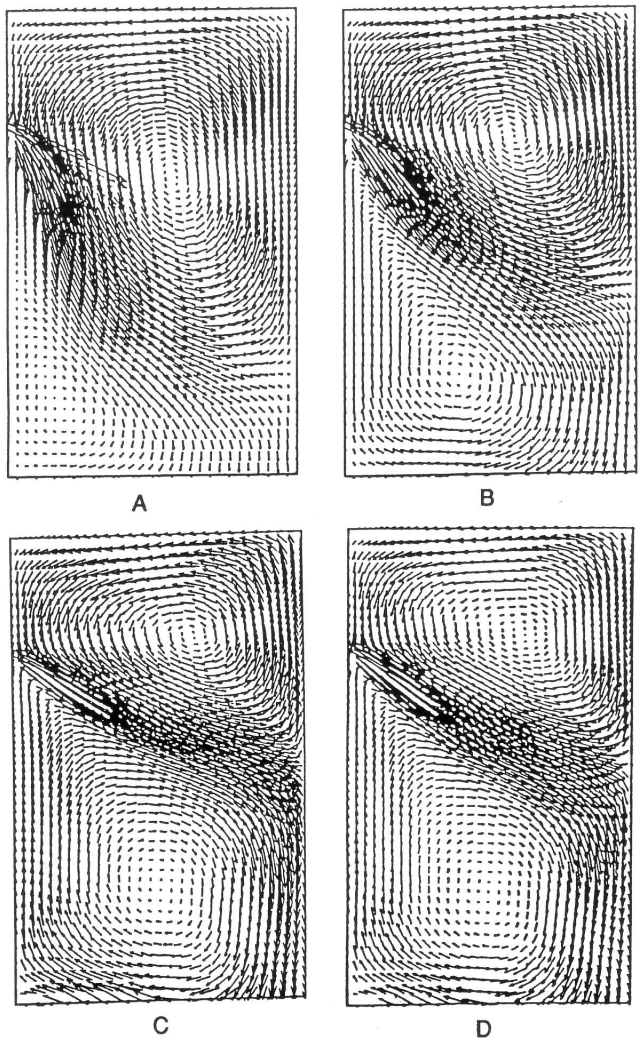

Fig. 3 — Effect of K and ε inlet values on calculated velocities in the water model:

(A) K = 0.15 ε = 2.12
(B) K = 0.09 ε = 0.77
(C) K = 0.09 ε = 1.77
(D) K = 0.06 ε = 0.44

conditions for the turbulence model. Increasing kinetic energy, K, apparently steepens the downward flow of the fluid, while increasing dissipation, ε, has the opposite effect. The last frame (Figure 3D) employed the average K and ε values actually calculated across the exit port by the nozzle model. These values were employed as boundary conditions for the turbulence parameters in the "true" simulation of flow in the mold for this set of casting conditions.

In addition, the fluid velocities leaving the port, that are calculated by the nozzle mode and pictured in Figure 4, are used as the velocity boundary conditions across the inlet plane to the mold region. These are equally important, since the average fluid angle leaving the nozzle ports is rarely the same as the nominal angle of the edges of the nozzle ports. The findings shown in Figure 3, and past experience, show that careful attention to all modeling details, especially the boundary conditions, is essential to obtaining reliable simulation results.

Model Verification

An example of the flow distribution calculated by the nozzle model for a nominal 15 deg downward nozzle is shown in Figure 4. This figure shows that the velocity distribution over the nozzle outlet is skewed, with most of the fluid leaving the lower half of the nozzle port openings. The upper part is relatively stagnant, with some recirculating fluid actually *entering* the nozzle. Observations of the physical water model at Inland Steel confirm this finding. Because the flow across the top of the nozzle exit ports is very slow and into the nozzle, the nominal angle of the top edge of the exit port would not be expected to affect the flow. In fact, a water modeling study that varied the upper and lower nominal angles independently, has confirmed that the nominal angle of the upper edge of the outlet port has no effect on the average angle of the jet leaving the nozzle.[11]

To further verify acceptable accuracy of the model, predicted flow patterns within the mold region of the continuous caster were compared with experiments conducted using a Plexiglas water model of the process. By superimposing the calculated velocities on one-half of a photograph of the water flow pattern, Figure 5 illustrates a typical comparison, using casting conditions of 1.0 m/min, and nozzle angles of 15 deg up. The horizontal beam running across the photograph supports the Plexiglas faces of the water model and has no effect on the flow.

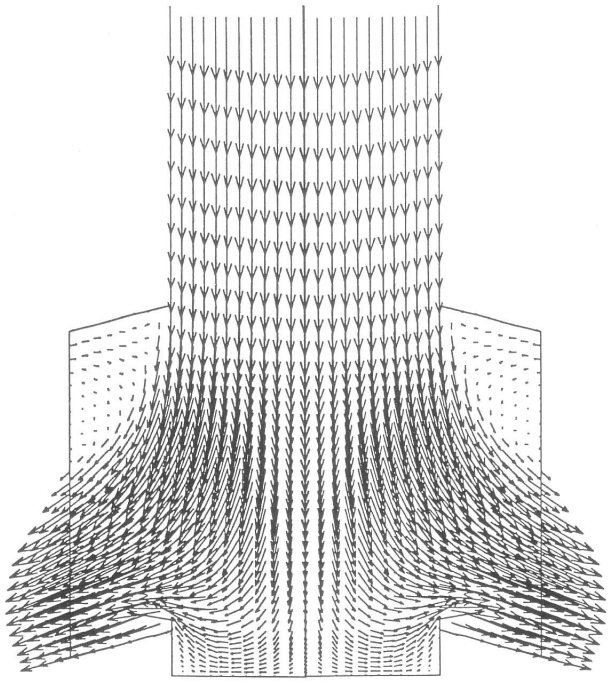

Fig. 4 — Flow within the bifurcated nozzle, using a nominal outlet angle of 15 deg down.

The shape of the inlet jet plume, impingement point and overall flow characteristics observed in Figure 5 all show a general similarity. Both the observed flow pattern and the simulation show how the jet spreads outward until it impinges against the narrow face. It then spreads in all directions, with the bulk of the flow splitting either downward or upward to the meniscus to flow back along the free surface to the nozzle. The result is four slowly recirculating zones, all of which eventually bring fluid back to the nozzle. Both models exhibit a jet in the mold angled at approximately 20 deg downward.

Figure 5 also shows how flow from a nominally 15 deg upward facing nozzle still produces a downward jet in the mold region of the caster. In fact, both mathematical model simulations and observations of the physical model consistently showed that, for the nozzle configurations studied, the flow always leaves the nozzle at a downward angle, regardless of port orientation. The flow angle is larger than the port angle. This effect is attributed to the downward momentum of the fluid. It has also been noted by other investigators, using both physical[12] and mathematical[13] models. Table I summarizes the effect of varying nozzle angles, while at the same time comparing the observed and calculated jet angles. The general agreement between the results generates confidence that the two-dimensional model is capable of making reasonable flow predictions in an actual continuous caster.

Figure 6 shows a comparison between the flow patterns predicted in the physical water model, with flow from its bottom restricted at 1.12 m deep, and the top portion of an actual caster (using steel properties and an unconstrained outlet condition on a 3 m long model domain). The velocity solution for steel generally resembles the flow patterns obtained in water model simulations. This was expected, owing to the large

Table I — Comparison of Estimated Jet Angles Observed in the Mold Interior

Nominal Inlet Angle	Physical Model	Mathematical Model
30 deg up	—	15 deg down
15 deg up	20 deg down	20 deg down
0 deg (horizontal)	—	25 deg down
15 deg down	35 deg down	30 deg down
25 deg down	40 deg down	—
30 deg down	—	35 deg down

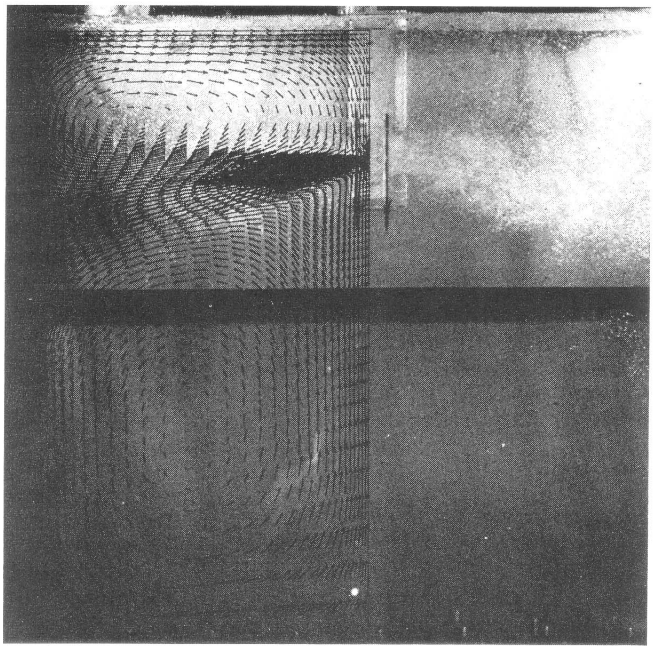

Fig. 5 — Comparison of calculated and measured flow patterns in the water model using 15 deg upward angled nozzles.

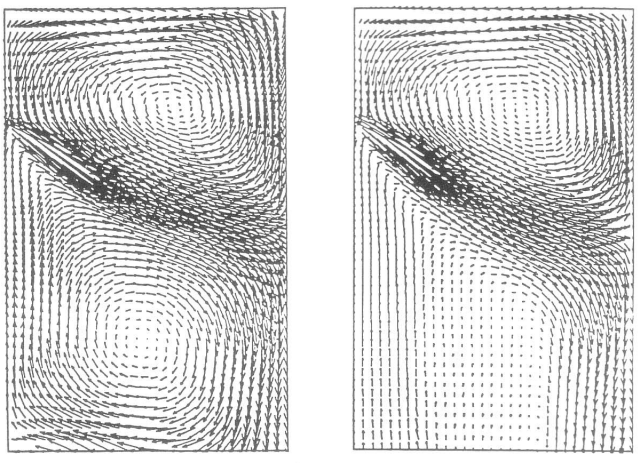

Fixed Bottom Open Bottom

Fig. 6 — Comparison of calculated velocities in the 1.12 m water model with a fixed Plexiglas bottom and the 3 m model with an open bottom (15 deg downward nozzles).

amount of successful experience using physical water models to predict flow in turbulent systems involving molten steel.

In a full-scale model, where the mold geometry (characterized by length D) and inlet velocities, V, are made the same as those in the actual caster, the *kinematic viscosity, ν*, controls the similarity parameter, Reynolds number, (VD/ν). This fluid property is 0.95 for water and 0.78 for steel. The 18 percent difference was found to have very little effect on the flow pattern. This was expected, since changes in the Reynolds number do not greatly affect the flow if it is fully turbulent.

Of much greater importance is the Plexiglas bottom required in the physical model. The bottom of the physical water model significantly affects the fluid flow patterns in the lower recirculation zone of the physical model. The shorter model prematurely forces fluid moving vertically down the narrow face walls to flow back toward the center, where it recirculates up toward the nozzle. Although this does not significantly affect the jet angle, it might affect the distribution of entrained particles in inclusion particle distribution studies. Simulations were performed using model domain lengths varying from 1.1 to 6.0 m with the outlet normal (vertical) velocity unconstrained. These results (see Figure 7 for an example using a 3 m long model) determined that recirculation extends to substantial depths below the mold in the caster and the flow does not become uniformly downward until almost 6 m deep in the strand. The minimum length required for accurate flow simulation using a physical model actually depends on the casting conditions. Greater widths, higher casting speeds and steeper downward pointing nozzle angles would all require a longer physical model.

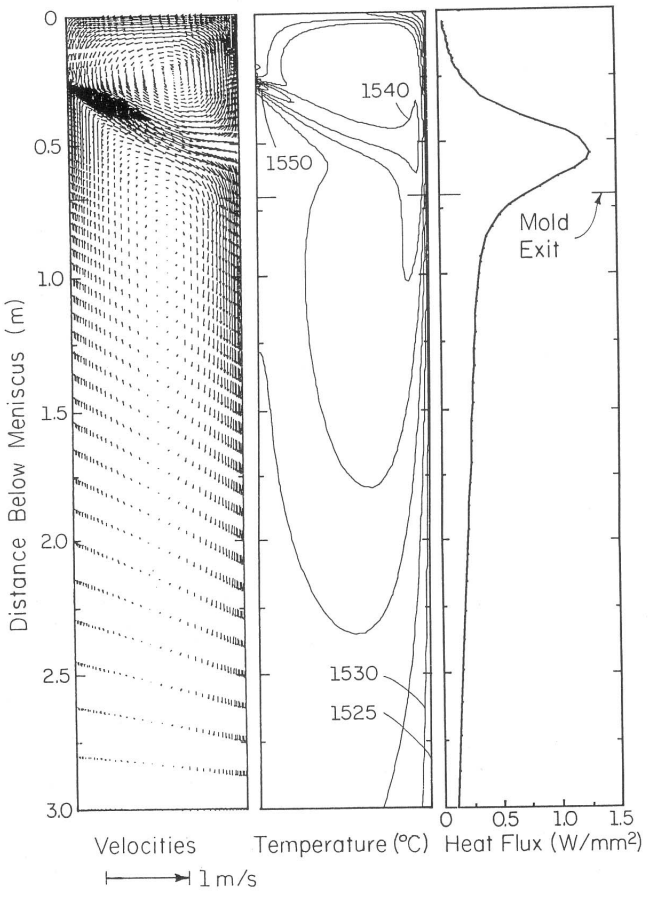

Fig. 7 — Calculated velocity, temperature and narrow face heat flux (for a 1.0 m/min and 15 deg downward nozzle).

Example Application to Shell Thinning

The superheat in the fluid steel can be convected to the shell, and conducted through the shell to the copper mold walls, or it can be swept out of the mold region, to be dissipated much lower in the caster. In addition, the delivery of superheat to the shell is uneven, and will produce a maximum heat input near the point of jet impingement. This can produce local "hot spot(s)" on the shell, where growth is slow, and may cause shell thinning, erosion and even lead to breakouts, particularly at higher casting speeds.[14] Equally important is the influence of the flow pattern on the temperature of the steel delivered to the meniscus. If the steel temperature is too low during the critical solidification stage, it is believed to exacerbate defect formation.[12]

To investigate this behavior, the mathematical model was extended to calculate the temperature distribution resulting from the previously calculated velocity flow distributions. Figure 7 presents an example of the temperature contours in the liquid pool, adjacent to the corresponding velocity distribution from which it was calculated, for a 1.0 m/min casting speed and 15 deg downward nozzle. The isotherms clearly outline the path of the hot steelmaking up the jet and show how the fluid carries heat to the narrow face wall, and then moves both upward and downward, cooling as it travels. By the time it reaches the meniscus, the fluid steel has cooled considerably, which makes freezing over of the meniscus more likely. This, in turn, may produce deeper meniscus marks which could have important implications on steel quality and subsequent crack formation.

Figure 7 also presents the corresponding relative heat flux across the liquid/solid shell boundary calculated as a function of distance down the narrow face wall. It shows that heat input to the shell is at maximum near the bottom of the mold at the region where the jet impinges upon the wall. This behavior is logical and has been found to coincide with a reduction in the shell growth rate.[14]

This finding has important implications. If the maximum in heat flux were allowed to move beneath the level of mold exit, then the peak heat flux to the inside surface of the shell could occur opposite the minimum in heat extraction from the outer shell surface, since the water sprays just below the mold are less efficient. The result would be surface reheating, accompanied by shell thinning due to erosion. The combination would increase the likelihood of a breakout through the less well-supported, narrow face shell just below mold exit, where the shell is its thinnest, hottest and weakest. This problem is most likely at higher casting speeds, and with steeper downward pointing nozzles. It should be noted that casting speed is effectively doubled if one of the ports becomes blocked from alumina buildup, so potential problems exist even at "safe" casting speeds.

Summary
A mathematical model of fluid flow and heat transfer inside the shell of a continuous casting mold has been developed and verified with experimental observations and physical models. Even a two-dimensional model is able to simulate the process, if care is taken to incorporate the essential phenomena into the model. In this case, it was found to be extremely important to extend the simulation back upstream to include flow from the nozzle. The model was found to predict and explain many experimentally observed phenomena, in addition to providing new insights into, for example, the differences between physical water models and steel casters. The model has then been applied to briefly explore the potential defect of narrow face shell erosion by impingement of the steel jet. This application and many others deserve future work with this model. These include the behavior of inclusions, the details of heat delivery to the meniscus area and the effect of electromagnetic braking. Combined with other models, to be discussed in the next sections, the results of this work should increase our understanding of the early stages of shell solidification in the mold and eventually provide insights that will aid in the prevention of breakouts and other quality problems.

THERMAL DISTORTION OF THE MOLD

Thermal distortion of the mold tube has been found to be extremely important to quality in the continuous casting of steel billets, which has been the subject of extensive investigation.[15-17] In contrast, very little effort has been expended to understand the distortion of continuous slab casting molds. Perhaps this is because little *residual* distortion has been observed in slab molds. However, significant distortion of the mold is possible during operation at elevated temperatures without measurable residual distortion of the mold when it returns to ambient temperature. Residual distortion is found only when significant plastic deformation at operating temperature is allowed by the constraint system. Since the size of the air gaps that form in the corner regions of the slab are very small (on the order of only a few tenths of a millimeter), even a small mold distortion can have a significant impact on heat transfer from the shell to the mold. To investigate the mechanical behavior of the continuous slab casting mold during operation, a three-dimensional finite-element, thermal stress model of a typical slab mold has been developed.[18]

Model Formulation

The model calculates the temperature, displacement and stress distributions in one-quarter of a typical slab casting mold (assuming two-fold symmetry), under steady-state operating conditions. Figure 8 shows the three-dimensional finite-element mesh used in the simulation and Figure 9 shows the boundary conditions for a transverse section. The cooling water chamber has been modeled as a simple 3 cm thick steel backing plate, so it neglects some of the stiffening effect of the box actually used. The configuration shown here has the end plates positioned for casting 36 in wide slabs. Heat is input to the exposed surfaces of interior mold elements as a function of distance

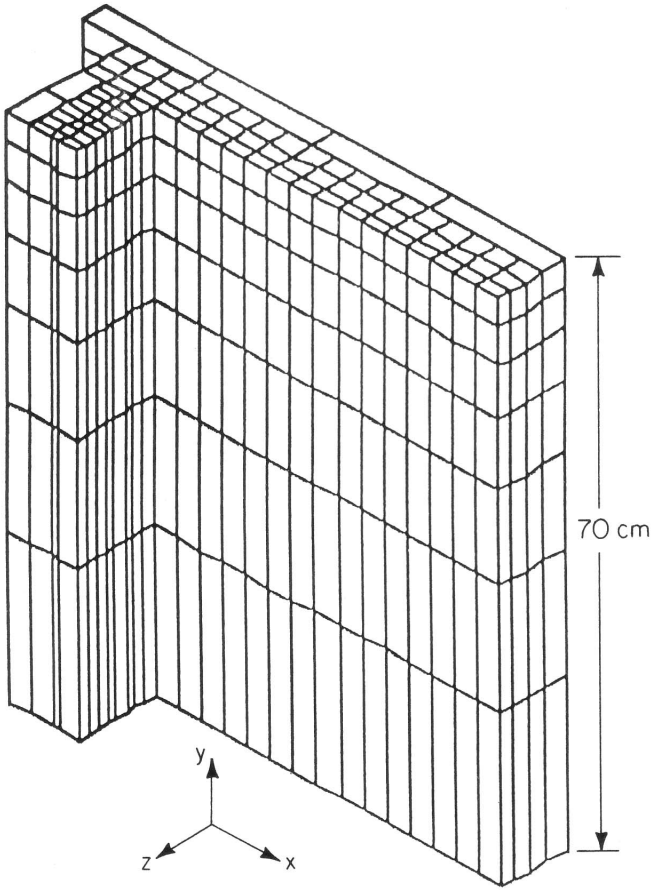

Fig. 8 — Finite-element mesh used in three-dimensional thermal stress analysis of the slab mold.

down the mold by applying heat flux values derived from previous measurements (shown in Figure 15).[19] Cooling water channels, represented by convective heat transfer surfaces, extract heat from appropriate element boundaries *within* the mold. The finite-element form of the steady-state heat conduction equation is then solved throughout the domain to calculate the temperature distribution throughout the mold under operating conditions.

To perform the stress calculations, the mesh in Figure 8 is divided into four separate meshes, for the narrow face copper end plate, the wide face copper and the two steel backing plates, which are coupled mathematically only at those points where they connect mechanically in the genuine caster during operation. Mathematically, the end plate is made to "touch" the wide face at only two points on the inside corner and the copper wide face is "bolted" at several locations to the backing plate. Thermal expansion loads are then applied to each node in the domain, based on the previously calculated temperature increases from the ambient temperature of 35 °C. Loads representing one side of the mold clamping forces are applied at the two appropriate locations on the exterior of the backing plate, as shown in Figure 9, and ferrostatic pressure loads are applied over the inside surfaces. As in all finite-element stress models, displacements are calculated by solving the equilibrium differential equations, and strains and stresses are derived subsequently, if desired. The equations for steady-state heat conduction and elastic thermal stress analysis

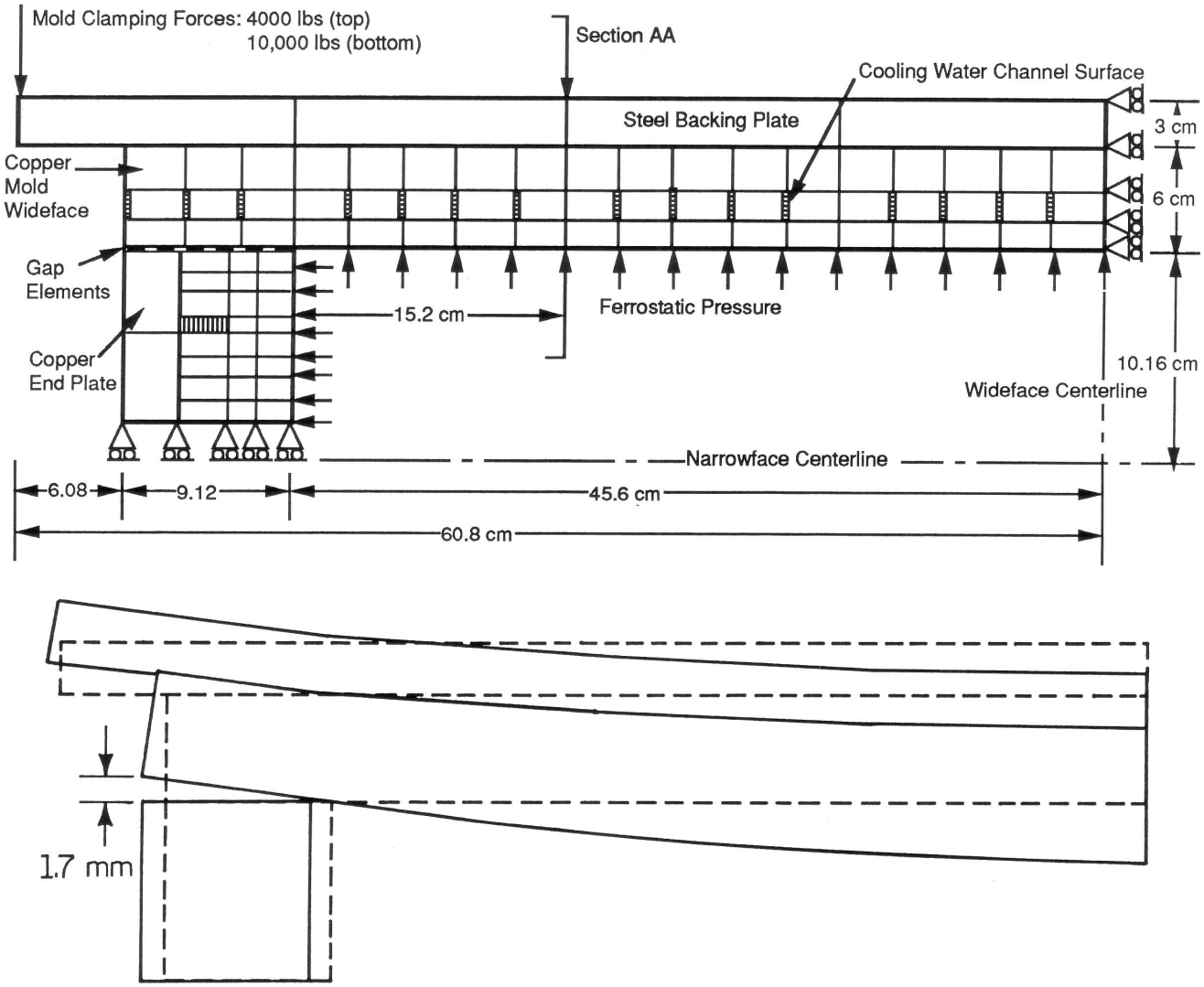

Fig. 9 — Model boundary conditions and distorted shape of a transverse section through the middle of the mold.

are both solved using the ANSYS finite-element code[20] and typical simulations require about 30 min to run on a Ridge 32 workstation.

Sample Results

Figure 9 shows the distorted shape of the mold, calculated by the model and exaggerated 10X, compared with the original outline. Figure 10 shows the corresponding temperature profile calculated through the mold thickness just below the meniscus. Both the temperature and displacement calculated along the mold surface are plotted in Figure 11 as a function of distance down the mold. Insight can be gained into the behavior of the mold during operation by understanding these results together with consideration of the mold construction and the constraint system.

A linear temperature gradient (characteristic of steady-state one-dimensional heat flow) is established within the solid portion of the copper plates, as shown in Figure 10. The *hot face* against the solidifying shell heats to over 300 °C, while the cooling water channels keep the *cold face* and the entire steel backing plate at or below roughly 100 °C. This is typical of the values measured in practice and agrees with previous model predictions.[19]

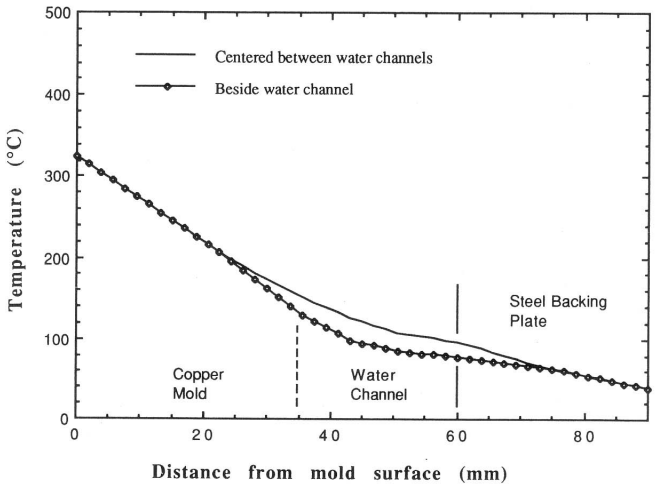

Fig. 10 — Temperature distribution through mold thickness (at the center of the wide face).

The hot face region of each copper plate attempts to expand more than its water-cooled outer region. In addition, the copper plate is constrained by the cold, stiff steel backing plate to which it is bolted. These effects force the entire wide face to bend inward, acting like a bimetallic strip in both the vertical and

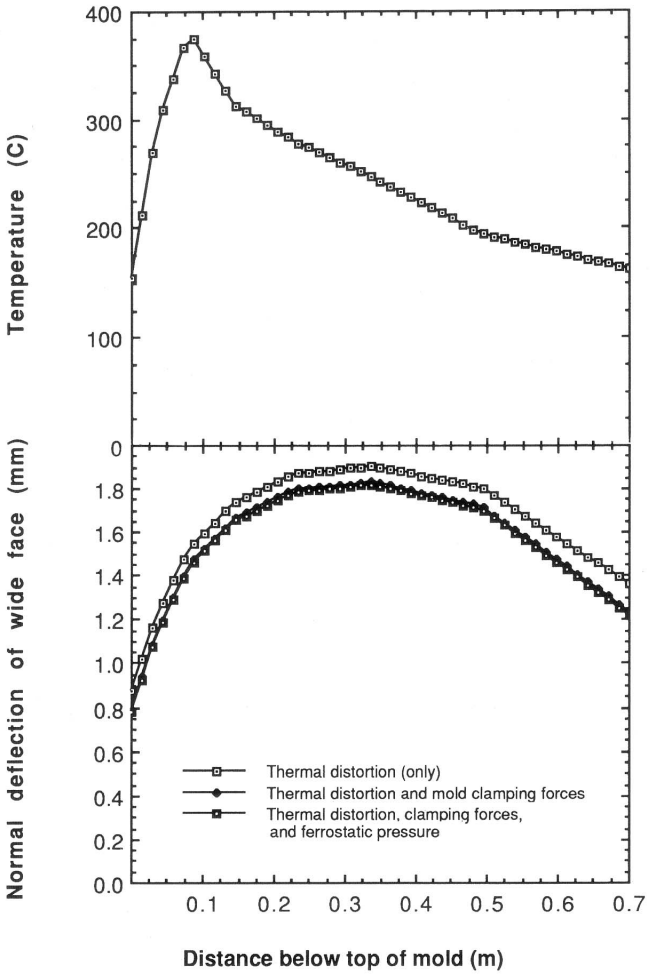

Fig. 11 — Temperature and distorted shape of the mold hot face surface (along section AA through the off-corner of the wide face shown in Figure 9).

horizontal directions. The maximum distortion then occurs at the very center of the wide face, as indicated by Figures 9 and 11. In addition, stresses are produced with compression in the copper hot face offset by tension in the steel.

Since the narrow face is connected to the wide face only through pressure, the wide face is free to rotate around the inner corner of the end plate, which acts as a hinge. As shown in Figure 9, this opens up a gap between the back of the end plate and the wide face which is crucial to producing the large distortions seen on the wide face. Calculations performed with the narrow face end plate rigidly attached to the wide face produced orders of magnitude less mold distortion.[18] This was because the dominant contribution to thermal distortion from bending due to the through-thickness temperature gradient was severely restricted.

It is interesting to note that the maximum distortion, which occurs halfway down the mold, does *not* correspond with the maximum temperature, which appears near the top of the mold, just below the meniscus. Since the separate plates of the slab mold distort due to bending, the maximum deflection is always found at the center of the plate. This is contrary to experience with the smaller, thinner billet molds, where the maximum distortion always coincides with the peak temperature.[16] The difference arises because the copper billet mold is a single unit and is not constrained by backing plates. When heated, it expands as a tube outward in all directions in proportion to its temperature, so the peak distortion is found near the meniscus. This illustrates the importance of mold construction and constraint system design to mold distortion behavior.

Figure 11 shows that the application of both mold constraining forces and ferrostatic pressure partially offsets the substantial thermal distortions predicted during operation. However, the restraining effect of the clamping forces, which were chosen to be the maximum likely ever used in practice, is still very small and the effect of ferrostatic pressure is negligible compared with the powerful forces of thermal expansion. Figure 11 also shows that there is more expansion at the bottom of the mold than at the top. This is because the higher heat input to the top of the narrow face copper makes it expand slightly more at the top than at the bottom. By pushing away the inner corner of contact with the wide face, bulging of the wide face is then offset slightly.

Because the copper mold is rigidly held against the backing plate, it is unlikely to exhibit much residual distortion after it cools to ambient temperature. However, there may be significant residual stress if the operating temperature is high enough to produce plastic flow due to creep in the copper.

Implications

The three-dimensional thermal stress model of the slab casting mold has predicted distortions during operation on the order of a few millimeters. The actual magnitude of mold distortions encountered in a given caster will depend critically on the stiffness of the cooling water chamber attached to the copper. Since the present calculations used a relatively flexible steel backing plate, compared to the thick, constraining cooling chambers found in most casters, actual mold distortions are likely to be less than those presented here. Even so, the relative trends predicted by the model should remain valid, and provide valuable insight into mold behavior during operation.

Even a small mold distortion could have a significant effect on heat transfer from the growing shell. Combined with the mold taper and shrinkage of the solidifying steel shell, this distortion affects formation of the air gap. The most important measurement in this regard is not the total distortion of the mold faces, but rather the *difference* between the distorted mold position at the meniscus, where the shell first forms, and the distorted positions down the rest of the mold. Figure 11 shows that this difference increases from zero at the meniscus to a maximum of 0.5 mm halfway down, to roughly zero again at mold exit. This creates a slight *negative taper* over the bottom half of the mold, which may contribute to the reduced heat transfer always observed in the lower portion of the mold. This distortion may also contribute to generating tensile stresses, important to crack sensitive grades. In the center regions of the mold, the thin shell must bend first inward, and then outward, to navigate around the bulge in the center of the mold. Increasing problems due to mold distortion via this mechanism would be expected with wider

slabs, since the larger distance between the end plates would allow more wide face bending distortion.

In the casting of thin sections, which has been the focus of much recent research on net shape casting processes, mold distortion will have an additional important effect on the final dimensions of the cast product itself. Without a great deal of rolling to control the final product gauge, these processes must rely on the accurate prediction and control of the temperature and shape of the casting and mold surfaces. If these processes are ultimately to succeed, mathematical models, such as the ones discussed here, will likely play an important role in their development.

HEAT FLOW AND STRESS MODEL OF THE SOLIDIFYING SHELL

Although the continuous casting process has been modeled extensively, only a few previous models have considered stress generation in slab casting machines.[21-23] Due to the complexity of the problem, it is only now becoming possible to incorporate into a mathematical model the known physical and mechanical phenomena that govern this coupled thermal/deformation process.

The formation of defects in continuously cast steel slabs is determined greatly by the behavior of the thin, growing shell during the early stages of solidification in the mold. During this time, the shell shrinks away from the mold near the corners due to thermal contraction. This forms a gap between the mold and strand, which causes the local rate of heat flow to diminish dramatically. The extent of this gap depends on the shrinkage of the thin shell, its strength to withstand the ferrostatic pressure pushing it outward, the casting speed, the mold flux heat transfer characteristics, mold distortion and the amount of mold taper present to offset the shrinkage. Of these variables, the mold taper is perhaps the most easily altered and directly controllable. With improper taper, the combination of bulging (where there is too little taper) and compression (where there is too much taper) may distort the shell and even form cracks or breakouts while it is weak and possibly fragile.

Model Description

To simulate the complex phenomena during solidification of the shell in the mold region, a two-dimensional, transient, heat transfer and stress model, called CONCAST, has been developed recently at the University of Illinois. This computer program tracks the behavior of a transverse slice through a continuously cast section as it moves down through the slab casting machine. It attempts to incorporate most of those phenomena important to the formation of defects of a longitudinal nature. The model is being used to study quantitatively, effects such as varying mold taper, and to help understand how the various defects are formed. It consists of separate finite-element models for heat flow and stress generation that are coupled through the size of the interfacial gap. Details regarding the formulation of the model and solution procedure are described elsewhere,[24-28] so only a brief discussion will be given here.

Heat flow model — The heat flow model solves the transient, two-dimensional heat-conduction equation over the domain shown in Figure 12, using a finite-element formulation.[28] Because heat flow in the axial direction is negligible, and the defects of interest are primarily longitudinal and exhibit two-fold symmetry, only one-quarter of a transverse section through the slab is considered.

Like most other heat flow models, this model presently accounts for convection in the liquid pool by simply increasing the effective thermal conductivity for molten steel. This ignores the significant variation in heat flux down the mold wall with a maximum near mold exit that arises from the nozzle jet. Eventually, it is planned to incorporate results from the fluid

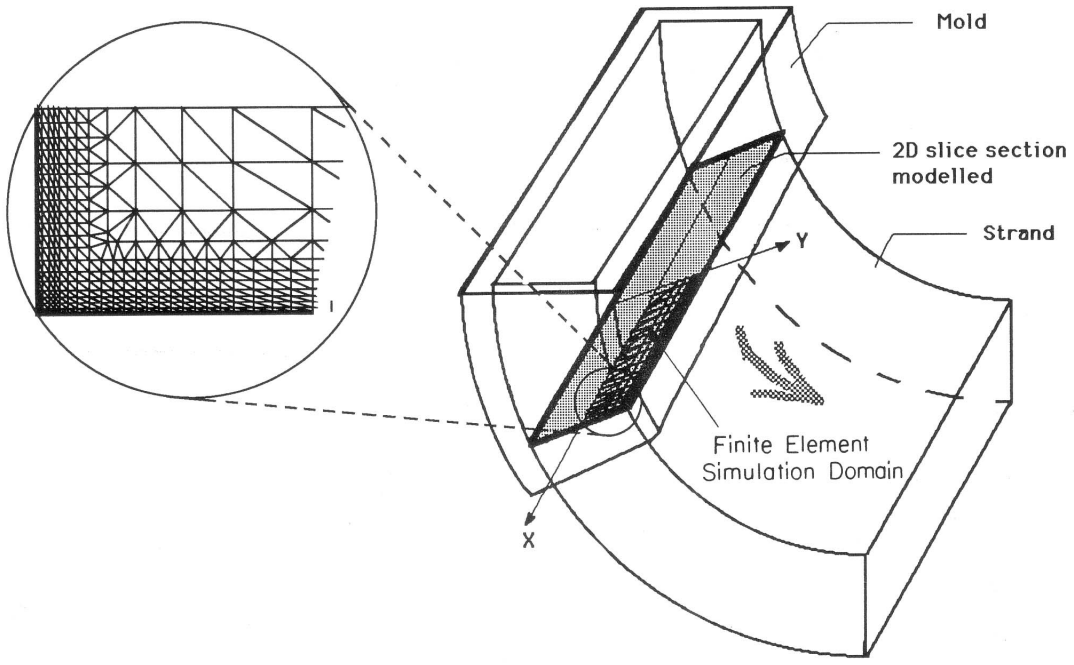

Fig. 12 — Schematic of a slab caster showing the transverse section simulation domain and mesh.

flow/heat flow model in the liquid pool previously discussed to provide better boundary conditions for heat flux to the solid/liquid interface of the present model, to take this effect into account.

Interfacial gap heat conduction model — The model results have been found to be quite sensitive to the heat transfer function employed across the interfacial gap between the shell and mold. The model currently uses a resistance to radiation in parallel with a series of four resistances to heat conduction, representing:

(1) Contact resistance between the mold and flux film
(2) Conduction through the flux film (assumed to increase in thickness from a minimum at the meniscus to a maximum as the flux cools and is based on the flux viscosity, melting rate and casting speed)
(3) Conduction through the air (or gas vapor) gap (where and when there is one)
(4) Contact resistance between the flux and the steel shell (if there is no air gap)

This heat transfer function is particularly sensitive to the thickness of the air gap that forms as the shell solidifies and shrinks away from the mold wall. The thickness of the gap is calculated at each location and time, knowing the position of the strand surface, calculated by the stress model at the previous time step and the position of the mold wall at that location and time. The latter can be found from previous mold distortion calculations and the original mold taper.

Stress model — The temperatures calculated by the heat flow model are then input to an incremental, two-dimensional, transient, elasto-visco-plastic, finite-element thermal stress model. The stress model is *stepwise coupled* with the heat flow model, as the solution alternates between the thermal and stress calculations as the slice moves down through the mold in successive time steps. At each time step, the load increments from the thermal strain are calculated from the temperatures generated by the heat flow model, using an input function for the thermal linear expansion. This is facilitated by use of the same domain and finite-element mesh (shown in Figure 12) for both the temperature and stress calculations.

The stress model includes a temperature-dependent elastic modulus, volume changes due to phase transformations, ferrostatic pressure and the resisting force of the mold walls. Plastic strain increments can be calculated from a plastic strain rate function that incorporates temperature-, stress-, strain- and time-dependent plastic behavior over the entire wide range of strain rate, temperature, strains and stresses encountered by the steel shell.[18] Mold oscillation and friction between the shell and mold are neglected.

One of the more difficult aspects of the modeling is to properly account for the restraining effect of the mold on the thin shell, deforming in the presence of internal ferrostatic pressure. To do this, gap elements are created between nodes on the surface of the solidifying shell and the mold wall. Iterative checks are required at each time step to ensure that only nodes that attempt to move through the mold wall are restrained, and that nodes that "wish" to shrink away from the mold wall are unrestrained. Iteration is also required to ensure that the size of the gaps calculated by the stress model are consistent with those assumed by the heat flow model. Convergence difficulties can make the computational costs very large, and runs of 30 min on the Cray X/MP are required even for an elastic solution.

Example Application to Longitudinal Surface Depressions

Stainless steel slabs are plagued by 2 to 5 mm deep surface depressions or gutters that form just off the corner along the wide face of the slab (pictured in Figure 13) These are accompanied by bulging along the narrow face. This is an expensive problem because subsequent reheating operations require the surface to be ground completely flat. In plain carbon steel castings, this location often exhibits subsurface cracks as well. A research project is currently underway to use the mathmatical model to simulate temperature and stress development in the solidifying shell, and focus on the influence of mold taper on heat transfer and deformation of the shell in the critical corner region. The ultimate goal of the project is to increase the understanding of the mechanism of formation of these defects, and hopefully to find a taper design for the narrow face of the mold that more closely matches the natural shrinkage of the shell, in order to reduce stress and distortion and their related problems.

Results and Discussion

Typical results from the model are presented in Figures 14 through 16. This particular simulation was for a 203 × 914 mm 304 stainless steel slab cast with a superheat of 30 °C at 0.9 m/min on the Armco Butler caster.[29] It was performed using an "ideal" taper along the narrow face, after 5 s of cooling. The narrow face was allowed to shrink as it chose (after first solidifying against a rigid resisting wall) with heat transfer behaving as if a fortuitous continuous taper had been employed along the narrow face. This was done both to predict quantitatively, what such an "ideal" taper would be, in addition to providing insight into how the narrow face would behave, if such a taper were employed. It also demonstrates a capability of the mathematical model that would be very difficult to duplicate experimentally.

Due to computational difficulties, this particular run did not include either plastic behavior or the

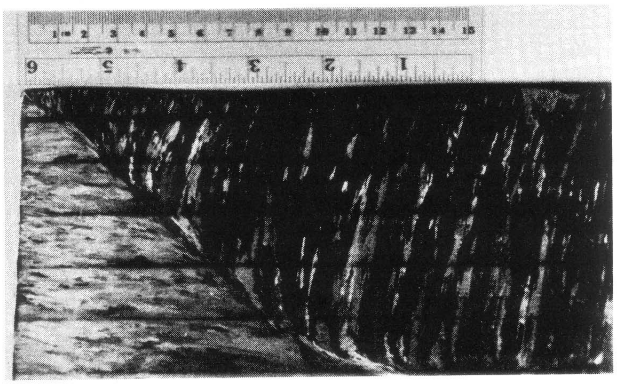

Fig. 13 — Photograph of the corner region of a 304 stainless steel slab showing off-corner surface depression or *gutter* along the wide face.

important results from the previous models:

(1) The effect of fluid flow causing uneven dissipation of superheat down the shell/liquid interface
(2) The influence of mold distortion on the position of the mold wall

Future runs plan to incorporate these effects.

Figure 14 shows the calculated temperature distribution in the shell at various times during cooling in the mold, along with the corresonding distorted shape, which is shown magnified 30X. An expected feature in this figure is that shrinkage of the corner region forms a gap that is accompanied by "hot spots" on the off-corner regions of both the narrow and wide face surfaces. These are the result of reduced heat flow across the large corner gap without the benefit of two-dimensional heat flow found at the corner itself. They correspond with a thinner shell in these regions and have been observed by previous researchers.[21, 23, 30] The effect is most pronounced along the narrow face where, at mold exit, the temperature increases from 1,040 °C at the middle of the narrow face to a maximum of 1,160 °C to less than 1,000 °C at the corner.

A second interesting feature in Figure 14 is the slight depression found just off the corner of the slab at 5 and 10 s. This phenomenon is due to rotation of the corner as the ferrostatic pressure pushes against the mid-narrow face and corresponds with a hot spot at the same location. The thinning of the shell that accompanies the hot spot on the wide face may be an important factor in the formation of defects, including off-corner gutters and breakouts. The depression disappears by the time the slab exits the mold.

As shown in Figure 15, the model used for calculating heat flow across the gap, combined with the gap calculations from the stress model, predicts heat fluxes that agree with experimental measurements previously performed on this slab caster by Samarasekera and Brimacombe.[19] It was interesting to find that the interfacial gaps predicted along the wide face are very thin. Ferrostatic pressure apparently maintains very close contact between the long, thin shell and the mold wall over most of the wide face. Since movement of the wide face shell also affects the narrow face, this finding implies that wide face taper is also important in determining how the narrow face shrinks.

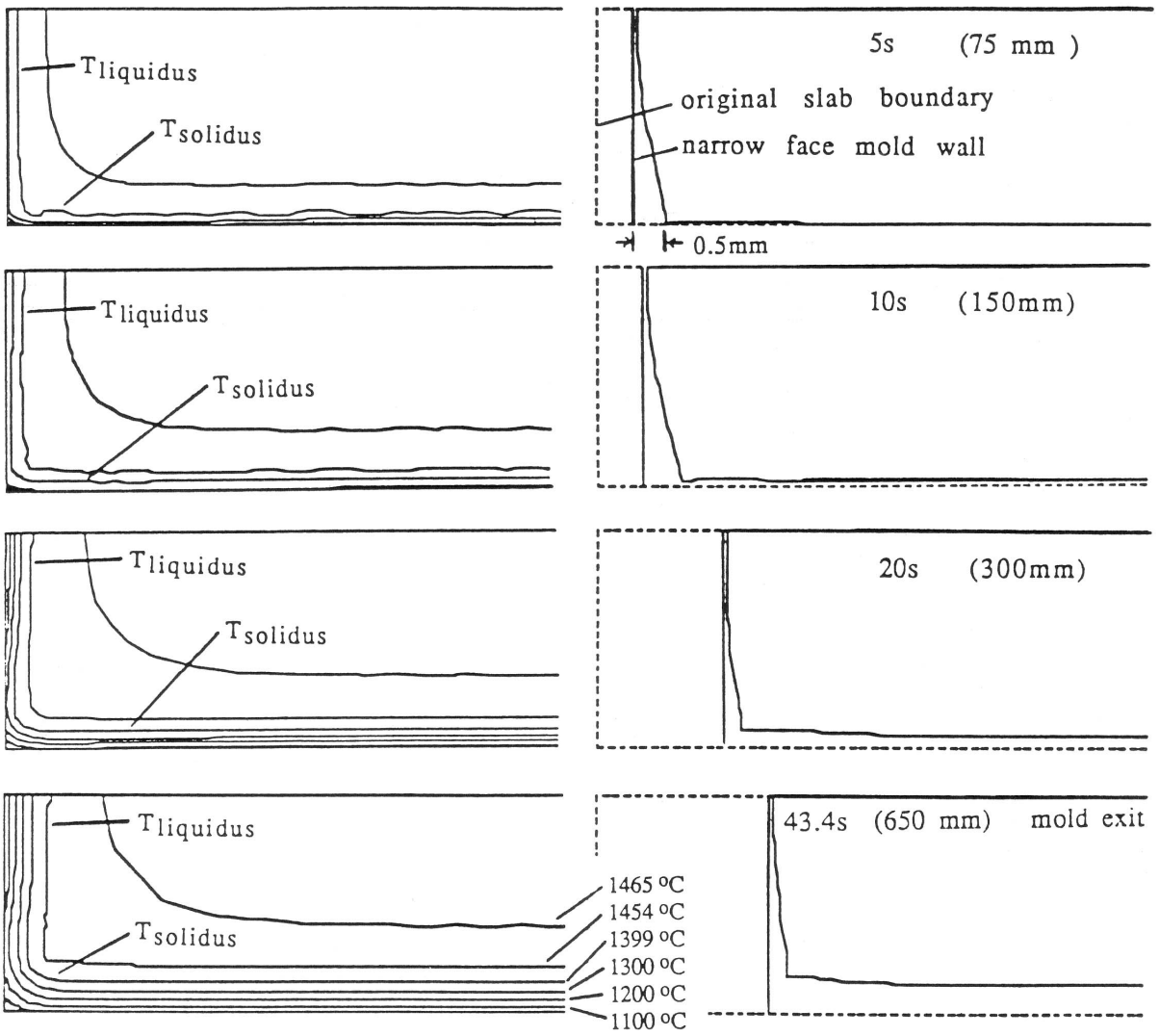

Fig. 14 — Calculated temperature contours (°C) and corresponding distorted slab shape (magnified 30X) at various times in the mold (using *ideal taper* along the narrow face).

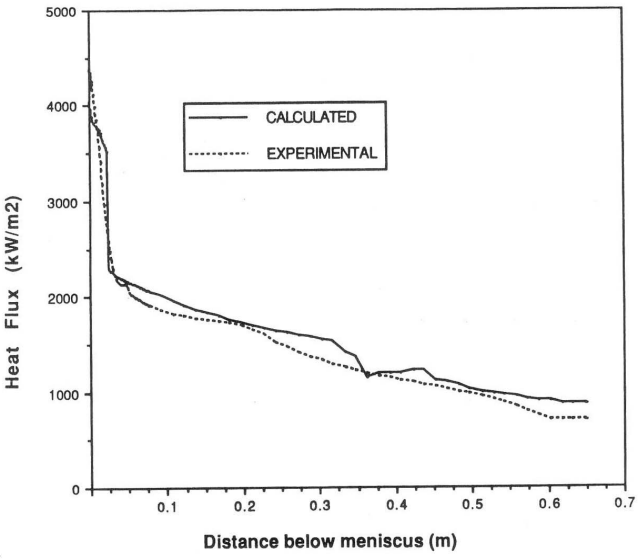

Fig. 15 – Comparison of calculated and measured[19] heat flux down the mold.

Figure 16 presents a plot of shrinkage at the center and corner of the narrow face for this ideal taper run. The 1.15 percent/m linear taper of the end plates currently employed, is included for comparison. This figure shows that the linear taper is a fairly close approximation of how the narrow face desires to shrink. However, it allows the formation of a large gap at the top of the mold, while at the bottom the mold wall pushes against the shell. A final note is that the extent of this non-linearity in narrow face shrinkage, predicted using the two-dimensional coupled model, is much less than that found with a simpler one-dimensional shrinkage calculation.[31]

Mechanism of Surface Depression Formation

Figure 17 postulates a mechanism contributing to the formation of off-corner surface depressions. The model

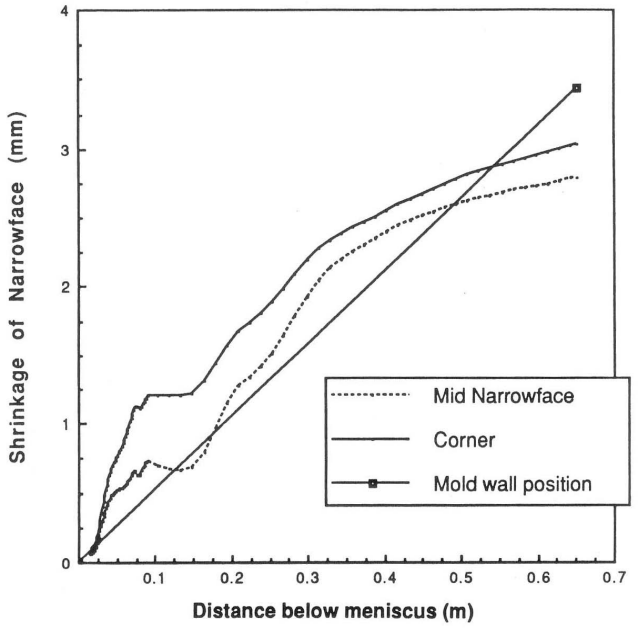

Fig. 16 – Calculated position of the narrow face (middle and corner) using *ideal taper,* compared with actual wall position (assuming a 1.15 percent/m taper).

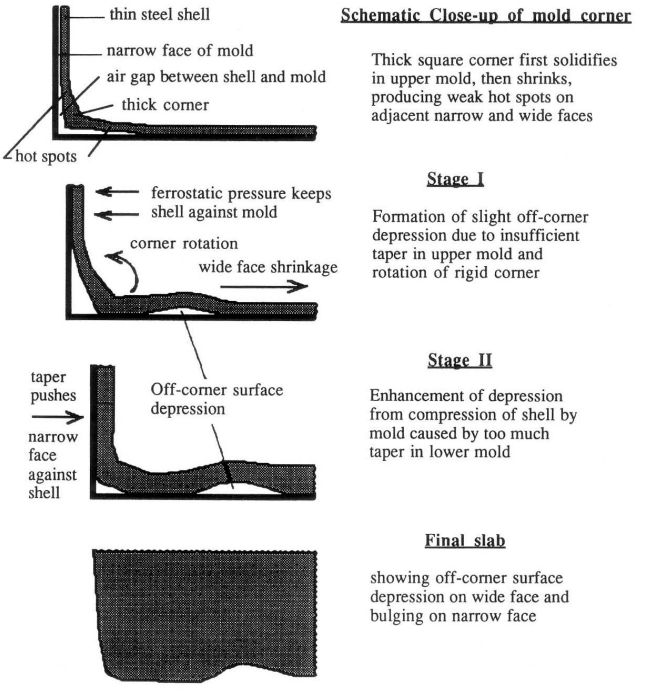

Fig. 17 – Suggested mechanism of the formation of the off-corner surface depressions.

results indicate that near the top of the mold, a simple linear taper cannot compensate for the rapid shrinkage of the wide face. While the wide face shrinks, the narrow face shell is held against the mold by ferrostatic pressure, so the shell opens up a relatively large air gap near the corner along the narrow face. This forces the narrow face shell to reheat near the corner. It also causes the shell to rotate slightly about the rigid solidified corner. This produces a slight depression close to the corner which results in reheating of the region adjacent to the corner region along the wide face as well. A mechanism similar to this is believed to be responsible for off-corner internal cracks in billets.[32]

Further down the mold, wide face shrinkage is less and the linear taper forces the narrow face wall to impinge on the shell, producing a compressive stress in the shell along the wide face. If this compressive stress is high enough, the shell will buckle slightly at its weakest point, which is the thinned region off the corner of the wide face where the small depression is already present. This will enlarge the surface depression.

This mechanism has not, as yet, been verified fully by the model predictions. The relative importance of the above two steps and other factors, such as further bulging below the mold, is not known. Further enhancement and validation of the mathematical model and additional runs are required to refine this mechanism and improve the model predictions in preparation for industrial trials using end plates designed with an optimized mold taper.

Other Applications

With only slight modification, these models can be applied to many other problems. In the mold, meniscus marks and transverse crack formation could be

studied by considering a *longitudinal* plane section, and incorporating solidification of the flux rim, mold oscillation and mold friction into the model. The model could also be extended down the caster to gain insight into other areas. These include the prediction of optimum *machine* taper as a function of operating practice, and determination of the relative importance of thermal and mechanical stresses in the spray and unbending regions. The latter is of great importance to the formation of transverse cracks, when tensile stresses at the surface are accompanied by low ductility in the critical 700 to 900 °C temperature range. The stress calculation is complicated by rapidly changing temperatures between roll segments, volume expansion due to the phase transformations that are delayed by precipitation kinetics and creep bulging under ferrostatic pressure.

Even beyond the caster, the models can be important in predicting temperatures and stresses during the slab transfer and reheating stages. As more products are pushed through the hot charging route, the potential exists for defects similar to those encountered during ingot casting. For example, panel cracks in microalloyed 0.1 to 0.2 percent C, high Mn grades containing aluminum are opened up by tensile stresses caused by the reversing temperature gradients arising during reheating after an intermediate amount of air cooling.[33] Some recent work has been done to investigate how and if they might also start to appear during the hot charging of continuously cast slabs of these grades.[34]

CONCLUSIONS AND FUTURE DIRECTIONS

Separate finite-element models have been developed to simulate fluid flow, heat flow within the mold cavity, mold distortion and shrinkage of the solidifying steel shell of a continuously cast slab. These advanced mathematical models provide a tool which can be used to gain insight into phenomena important to the process, to understand various problems that affect slab quality and to evaluate suggested improvements. The models demonstrate an increasing ability to correctly predict known behavior and to provide new insights.

This work emphasizes that important interrelations exist between the variables that control this complex casting process. Such diverse factors as nozzle design (which affects heat convected by fluid flow) and mold support and taper (which affects mold distortion and air gap formation) have important effects on solidification of the thin steel shell that are crucial to the quality of the final slab. These could be overlooked when focusing on specific aspects of the process isolation. Thus, it is desirable to link these models together, integrating the fluid flow, heat transfer and stress calculations. This work has already begun, with the coupling together of fluid flow, heat flow and stress models of the mold and shell of a continuous round caster.[35]

In the future, the fluid flow, heat transfer and stress models should be combined with microstructural models to predict metallurgical phenomena such as precipitation, recrystallization and segregation. In principle, this is straightforward, since these phenomena are determined by the temperature, stress and strain histories of the metal, which are already being predicted. In fact, these phenomena are not well quantified and themselves affect the stress history, so they will create further computational difficulties. Achieving these goals, and extending the range and accuracy of their predictions, will make mathematical models increasingly useful in understanding the continuous casting process.

Despite the many phenomena that are still not fully understood, continuous slab casting is a relatively mature process, which makes it the ideal proving ground for advanced mathematical models. These models will likely become even more important in the development and refinement of new casting processes, such as near-net-shape, thin slab and strip casting.

ACKNOWLEDGEMENTS

I wish to thank graduate students, Larry Mika, Bill Storkman, Jean Azzi, Glen Haegele and Fady Najjar, who did much of the work on the projects described in this paper. This research was made possible through the support of Inland Steel, Armco Inc. and Bethlehem Steel, which is gratefully acknowledged. I also thank Inland Steel and Armco Inc. for providing industrial data, Fluid Dynamics, Inc. for help with the FIDAP code and the National Center for Supercomputing Applications for providing time on the Cray X/MP computer.

References

1. B.E. Launder and D.B. Spalding, *Mathematical Models of Turbulence,* Academic Press, London, England, 1972.
2. R.I.L. Guthrie, "Physical and Mathematical Models for Ladle Metallurgy Operations," *Mathematical Modelling of Materials Processing Operations,* Edited by J. Szekely, L.B. Hales, H. Henein, N. Jarrett, K. Rajamani and I. Samarasekera, *TMS Conference Proceedings,* Palm Springs, CA, November 29, 1987, pp. 447-482.
3. Y. Sahai, "Computer Simulation of Melt Flow Control due to Baffles with Holes in Continuous Casting Tundishes," *Mathematical Modelling of Materials Processing Operations,* Edited by J. Szekely, L.B. Hales, H. Henein, N. Jarrett, K. Rajamani and I. Samarasekera, *TMS Conference Proceedings,* Palm Springs, CA, November 29, 1987, pp. 431-445.
4. O.J. Ilegbusi and J. Szekely, "The Modelling of Fluid Flow, Tracer Dispersion and Inclusion Behavior in Tundishes," *Mathematical Modelling of Materials Processing Operations,* Edited by J. Szekely, L.B. Hales, H. Henein, N. Jarrett, K. Rajamani and I. Samarasekera, *TMS Conference Proceedings,* Palm Springs, CA, November 29, 1987, pp. 409-429.
5. F.G. Wilson et al., "Effect of Fluid Flow Characteristics on Nozzle Blockage in Aluminum-Killed Steels," *Ironmaking and Steelmaking,* Vol. 14, No. 6, 1987, pp. 296-309.
6. W. Rodi, *Turbulence Models and Their Application in Hydraulics — A State-of-the-Art Review,* University of Karlsruhe, Karlsruhe, Germany, 1980.
7. K. Spitzer, M. Dubke and K. Schwertfeger, "Rotational Electromagnetic Stirring in Continuous Casting of Round Strands," *Metallurgical Transactions,* Vol. 17B, No. 1, 1986, pp. 119-131.
8. M.S. Engelman, *FIDAP Theoretical Manual — Revision 4.0,* Vol. 1, Fluid Dynamics International, Inc., Evanston, IL, 1987.
9. B.G. Thomas and L.M. Mika, "Simulation of Fluid Flow and Heat Transfer Inside a Continuous Slab Casting Machine," *Second FIDAP Users Conference,* Evanston, IL, October 2-4, 1988.
10. L.M. Mika, "Simulation of Fluid Flow and Heat Transfer Inside a Continuous Slab Casting Machine," Masters Thesis, University of Illinois, Urbana, IL, 1988.

11. N.A. McPherson, "Continuous Cast Clean Steel," *Steelmaking Conference Proceedings,* Iron and Steel Society, Inc., Vol. 68, 1985, pp. 13-25.
12. A. Ferretti, M. Podrini and G. Si Schino, "Submerged Nozzle Optimization to Improve Stainless Steel Surface Quality at Terni Steelworks," *Steelmaking Conference Proceedings,* Iron and Steel Society, Inc., Vol. 68, 1985, pp. 49-57.
13. M. Yao et al., "Three-Dimensional Analysis of Molten Metal Flow in Continuous Casting Mould," *Steelmaking Conference Proceedings,* Iron and Steel Society, Inc., Vol. 68, 1985, pp. 27-34.
14. H. Nakato et al., "Factors Affecting the Formation of Shell and Longitudinal Cracks in Mold during High Speed Continuous Casting of Slabs," *Trans. Iron and Steel Inst. of Japan,* Vol. 24, No. 11, 1984, pp. 957-965.
15. I.V. Samarasekera and J.K. Brimacombe, "The Continuous Casting Mould," *International Metals Review,* No. 6, 1978, pp. 286-300.
16. I.V. Samarasekera and J.K. Brimacombe, "Thermal and Mechanical Behaviour of Continuous-Casting Billet Moulds, *Ironmaking and Steelmaking,* No. 1, 1982.
17. J.K. Brimacombe, E.B. Hawbolt and F. Weinberg, "Metallurgical Investigation of Continuous-Casting Billet Moulds, Part I, Distortion, Fouling and Wear," *Continuous Casting,* Iron and Steel Society, Inc., Vol. 2, 1984, pp. 73-84.
18. J.A. Azzi, "Preliminary Steps in the Development of a 3-D Thermal-Stress Model of Continuous Casting," Masters Thesis, University of Illinois, Urbana, IL, 1988.
19. I.V. Samarasekera and J.K. Brimacombe, "The Thermal Field in Continuous-Casting Moulds," *Canadian Metallurgical Quarterly,* Vol. 18, 1979, pp. 251-266.
20. G.J. DeSalvo and R.W. Gorman, *ANSYS,* Swanson Analysis Systems, Inc., Rev. 4.3, 1987.
21. A. Grill, K. Sorimachi and J.K. Brimacombe, "Heat Flow, Gap Formation and Break-Outs in the Continuous Casting of Steel Slabs," *Metallurgical Transactions,* Vol. 7B, 1976, pp. 177-189.
22. I. Ohnaka and Y. Yashima, "Stress Analysis of Steel Shell Solidifying in Continuous Casting Mold," presented at *Modeling of Casting and Welding Processes,* Engineering Foundation Conference, Palm Coast, FL, April 17-22, 1988.
23. K. Kinoshita, T. Emi and M. Kasai, "Thermal Elasto-Plastic Stress Analysis of Solidifying Shell in Continuous Casting Mold," *Tetsu-to-Hagane,* Vol. 65, No. 9, 1979, pp. 40-49.
24. B.G. Thomas, I.V. Samarasekera and J.K. Brimacombe, "Mathematical Model of the Thermal Processing of Steel Ingots, Part I: Heat Flow Model," *Metallurgical Transactions,* Vol. 18B, No. 1, 1987, pp. 119-130.
25. B.G. Thomas, I.V. Samarasekera and J.K. Brimacombe, "Mathematical Model of the Thermal Processing of Steel Ingots, Part II: Stress Model," *Metallurgical Transactions,* Vol. 18B, No. 1, 1987, pp. 131-147.
26. W.R. Storkman and B.G. Thomas, "Heat Flow and Stress Models of Continuous Casting to Predict Slab Shape," *Modeling of Casting and Welding Processes,* Engineering Foundation Conference, Palm Coast, FL, April 17-22, 1988.
27. G.T. Haegele, "Mathematical Modeling of Defect Formation during the Hot Charging of Continuously Cast Steel Slabs," Masters Thesis, University of Illinois, Urbana, IL, 1988.
28. B.G. Thomas, I.V. Samarasekera and J.K. Brimacombe, "Comparison of Numerical Modeling Techniques for Complex, Two-Dimensional, Transient Heat Conduction Problems," *Metallurgical Transactions,* Vol. 15B, No. 2, 1984, pp. 307-318.
29. G. Drigel and R. Sussman, private communication, 1987 and 1988.
30. R. Alberny et al., "La Lingotiere de Coulee Continue de Brames et son Bilan Thermique," *Revue de Metallurgie,* July and August, 1976, pp. 545-557.
31. T.B. Harabuchi and R.D. Pehlke, *Continuous Casting,* Iron and Steel Society, Inc., Vol. 4, 1988, p. 55.
32. R. Bommaraju, J.K. Brimacombe and I.V. Samarasekera, "Mould Behaviour and Solidification in the Continuous Casting of Steel Billets, Part III: Structure, Solidification Bands, Crack Formation and Off-Squareness," *ISS Trans.,* Vol. 5, 1984, pp. 95-105.
33. B.G. Thomas, I.V. Samarasekera and J.K. Brimacombe, "Investigation of Panel Crack Formation in Steel Ingots, Part II: Off-Corner Panel Cracks," *Metallurgical Transactions,* Vol. 19B, No. 2, 1988, pp. 289-301.
34. G.T. Haegele and B.G. Thomas, "Application of Mathematical Models to Investigate Defect Formulation During Hot-Charging of Continuously-Cast Steel Slabs," Final Report to the Engineering Foundation for Grant RI-A-86-4, September 1988.
35. J.E. Kelly et al., "Initial Development of Thermal and Stress Fields in Continuously Cast Steel Billets," *Metallurgical Transactions,* Vol. 19A, No. 10, 1988, pp. 2589-2602.